

UNIVERSITY OF CRETE



Department of Physics

Bachelor Thesis

***Measurement of the parameters of the Feedback Control System
for the pupillary reflex***

Author:

Thalassinakis Christoforos

Supervisor:

Prof. Iannis Kominis

Quantum Physics and Quantum Biology Lab at the University of Crete
Department of Physics

January 19,2023

Ευχαριστίες

Με την διεκπεραίωση αυτής της εργασίας θα ήθελα αρχικά να ευχαριστήσω τον επιβλέποντα καθηγητή Ιωάννη Κομίνη που μου έδωσε την ευκαιρία να αποτελέσω μέλος της ομάδας του και να εκπονήσω την διπλωματική μου εργασία στο εργαστήριο Κβαντικής Φυσικής και Κβαντική Βιολογίας. Μου έδωσε την ελευθερία να δοκιμάσω τις ιδέες μου, και μου έδειξε τι σημαίνει πειραματική φυσική.

Στην συνέχεια θα ήθελα να ευχαριστήσω όλη την ομάδα του εργαστηρίου και πρώτα απ' όλους τον Παναγιώτη Καραβέλα με τον οποίο περάσαμε αμέτρητες ώρες μαζί στο εργαστήριο. Νιώθω τυχερός που μπορώ να τον αποκαλώ συνεργάτη άλλα και φίλο μου. Επίσης θα ήθελα να ευχαριστήσω την Ιωάννα Δεμερίδου, Εμμανουέλα Χρυσάφη και τον Θανάση Μαχά για την συνεχή τους στήριξη και το ευχάριστο περιβάλλον στο εργαστήριο.

Τέλος, θέλω να πω ένα μεγάλο ευχαριστώ στην οικογένειά μου καθώς με στήριξε και πίστεψε σε εμένα καθ' όλη τη διάρκεια των σπουδών στο τμήμα Φυσικής.

Contents

[\(0\) Introduction](#)

[\(1\) Dynamical Control Systems and Feedback](#)

[\(2\) Simple forms of Feedback](#)

[\(3\) Transfer Function](#)

[\(4\) Stability](#)

[The General Nyquist Criterion](#)

[\(5\) Operational Amplifiers and Signal Processing](#)

[\(6\) Voltage Control Oscillator](#)

[\(7\) Voltage Variable Attenuator](#)

[\(8\) Low Noise Amplifier](#)

[\(9\) Circuit design and symbolic circuit analysis](#)

[\(10\) Measurements 1](#)

[Tuning \$k_i\$](#)

[Tuning Loop-Gain](#)

[Tuning \$k_i\(2\)\$](#)

[\(11\) Measurements 2](#)

[\(12\) Experimental set-up of the optical components 1](#)

[\(13\) Pulse repeatability](#)

[\(14\) Basic anatomy and function of the eye](#)

[Anatomy](#)

[Neural pathways](#)

[The constriction pathway](#)

[The dilation pathway](#)

[The pupil light response](#)

[Pupil reflex as a control system](#)

(15) Experimental set-up and measurements

(16) Pupillometry- Application in medicine and Challenges

Bibliography

(0) Introduction

The purpose of the Thesis was to make use of basic control system theory to (1): design a feedback control system for the intensity and the pulse type of a laser beam and (2): use that laser beam to measure the parameters of the feedback control system of the pupillary reflex.

(1) Dynamical Control Systems and Feedback

A dynamical system is a system whose response changes over time due to an external forcing or stimulation. If two or more dynamical systems are connected to each other while one system influences the other and their dynamics, then that strong couple is referred to as feedback. There are two basic terms that describe such systems, Open Loop and Closed Loop. If there is an interconnected cycle between the systems then we define a Closed Loop system but if that connection is broken we define the Open Loop configuration. We often use block diagrams to describe these systems as illustrated in the figure 1.1 below.

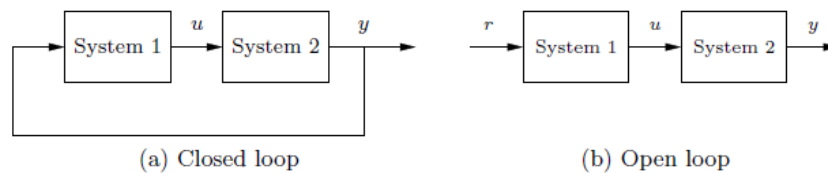


Figure 1.1: Open and closed loop systems. (a) The output of system 1 is used as the input of system 2, and the output of system 2 becomes the input of system 1, creating a closed loop system. (b) The interconnection between system 2 and system 1 is removed, and the system is said to be open loop.

In the case of an Open Loop system, in the presence of a disturbance, the corrective actions come after the error. But in some cases we are able to measure the disturbance before it influences the system and thus we are able to take corrective actions before the error occurs, by generating a control signal that counteracts it, this is also known as a *Feed-forward* system. We can make use of the block diagrams of Figure 1.2 to compare the *Feed-forward* and *Feedback* systems. Both systems have a reference signal r that indicates the desired output of the process P and a disturbance u . The Feedback system adjust the input of the Process through the Controller C , based on the measurement of the output y , so the output maintain the reference value. The feed-forward system measures the reference and the disturbance and provides the Process with the input that results in the desired output.

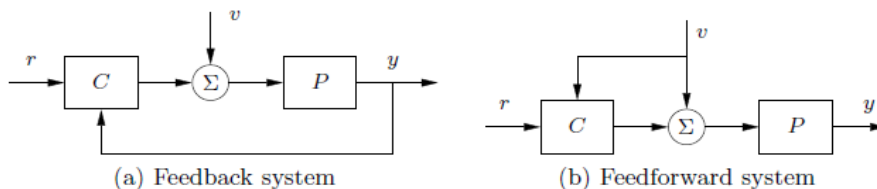


Figure 1.2: Feedback system versus feedforward system. In both systems we have a process P and a controller C . The feedback controller (a) measures the output y to determine the effect of the disturbance v , while the feedforward controller (b) measures the disturbance directly, but does not directly measure the process output.

The use of algorithms and feedback systems to achieve the desired outcome defines the Control, characterized by the central concept of the feedback loop of sensing, computation and actuation.

Figure 1.3 : Properties of feedback and feedforward

Feedback	Feedforward
Closed loop	Open loop
Acts on deviations	Acts on plans
Robust to model uncertainty	Sensitive to model uncertainty
Risk for instability	No risk for instability

(2) Simple forms of Feedback

On-Off Control

This type of control is described as follows:

$$u = \begin{cases} u_{max}, & \text{if } e > 0 \\ u_{min}, & \text{if } e < 0 \end{cases}$$

,where $e = y-r$ is the control error, the difference between the output and the reference signal (u indicates the actuation command). This simple system does not require any tuning since there are no parameters to tune but often results in oscillations since the system overreacts to small changes (which is often acceptable if their amplitude is small).

PI Control

The effect of oscillations of the On-Off control can be avoided with proportional control for small errors described as follows:

$$u = \begin{cases} u_{max}, & \text{if } e \geq e_{max} \\ k_p e, & \text{if } e_{min} < e < e_{max} \\ u_{min}, & \text{if } e \leq e_{min} \end{cases}$$

,where the controller gain is denoted as k_p . For this type of control the process variable often deviates from the reference signal since a non zero error signal is required to generate an input, even in the steady state. This deviation is also called steady state error. This effect can be avoided by making the control action proportional to the integral of the error:

$$u(t) = k_i \int_0^t e(\tau) d\tau$$

This type of control is called integral control with k_i the integral gain, which leads to zero steady state error. Combining integral and proportional control we derive the controller described as follows:

$$u(t) = k_p e(t) + k_i \int_0^t e(\tau) d\tau$$

The control action is the sum of two terms, the past by the integral of the error and the present by the proportional term. This type of feedback control is defined as PI-Control.

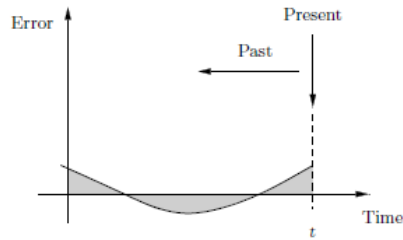


Figure 2.1 : Action of a PI controller. At time t , the proportional term depends on the instantaneous value of the error. The integral portion of the feedback is based on the integral of the error up to time t (shaded portion).

(3) Transfer Function

The transfer function is a function of complex variables, used to describe the dynamics of a system by the representation of its differential equations. The transfer function allows the correlation of the signals of complex systems represented by block diagrams using simple algebra. The transfer function is defined as:

$$H(s) = \frac{Y(s)}{X(s)}$$

,where $X(s) = \mathcal{L}\{x(s)\}$ (the Laplace transform of the input signal) and $Y(s) = \mathcal{L}\{y(s)\}$ (the Laplace transform of the output signal).

(4) Stability

For linear dynamical models the input/output behavior of the system can be represented by linear differential equations

$$\frac{d^n y}{dt^n} + a_1 \frac{d^{n-1} y}{dt^{n-2}} + \dots + a_n y = b_0 \frac{d^m u}{dt^m} + b_1 \frac{d^{m-1} u}{dt^{m-1}} + \dots + b_m u \quad (1)$$

where y is the output, u is the input and the coefficients a_k and b_k are real numbers. The equation above can be characterized by two polynomials

$$a(s) = s^n + a_1 s^{n-1} + \dots + a_n \quad \text{and} \quad b(s) = b_0 s^m + b_1 s^{m-1} + \dots + b_m$$

,where $a(s)$ is the *characteristic polynomial* of (1) and the related homogenous equation

$$\frac{d^n y}{dt^n} + a_1 \frac{d^{n-1} y}{dt^{n-2}} + \dots + a_n y = 0 \quad (2)$$

As a result we can derive the transfer function of the system

$$G(s) = \frac{b(s)}{a(s)}$$

When using feedback, it is important to make sure that the system remains stable. This means that if all the solutions to the equation (2) for the system go to zero for any initial condition, the system is stable. *This can only happen if all the roots of the characteristic equation*

$$a(s) = s^n + a_1 s^{n-1} + \dots + a_n = 0$$

,have negative real parts.

The General Nyquist Criterion

Before introducing the Nyquist criterion it is important to define the Nyquist contour and the Nyquist plot. The *Nyquist contour* Γ , of the Loop Transfer Function $L(s)$, encloses the right half-plane, while a small semicircle around the any poles of $L(s)$ at the origin is introduced, while an arc with radius R extends towards infinity. The Nyquist plot is the image of the $L(s)$ as s traverses Γ in the clockwise direction. The gain and phase for a frequency ω are

$$\text{Gain} = |L(i\omega)| \quad \text{and} \quad \text{Phase} = \angle L(i\omega)$$

Theorem. Consider a closed loop system with loop transfer function $L(s)$ that has $n_{p,rhp}$ poles in the region enclosed by the Nyquist contour. Let $n_{w,\Gamma}(1+L(s))$ be the winding number of $f(s)=1+L(s)$ when s traverses Γ in the counterclockwise direction. Assume that $1+L(i\omega) \neq 0$ for all ω on Γ and that $n_{w,\Gamma}(1+L(s)) + n_{p,rhp} = 0$. Then the closed loop system has no poles in the closed right half-plane and it is stable. If we let N be the number of clockwise encirclements of the point -1 , P be the number of unstable poles in the loop transfer function and Z be the number of unstable zeros of $1+L$ then:

$$Z = N + P$$

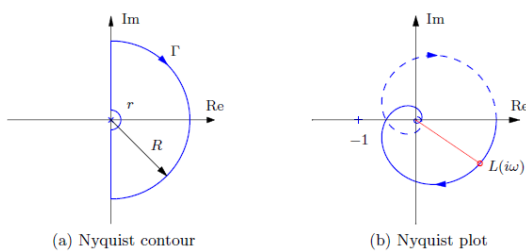


Figure 4.1: Nyquist Contour and Nyquist Plot

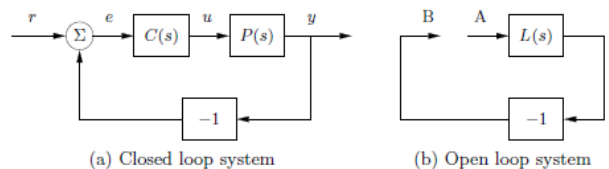


Figure 4.2: Block diagram of a Closed Loop and Open Loop system

Note: The loop transfer function L is simply the transfer function from the input at position A to the output at position B multiplied by -1 (to account for the usual convention of negative feedback), and as a result:

$$y = CP / (1 + CP) r = L / (1 + L) r$$

(5) Operational Amplifiers and Signal Processing

The OpAmp is a universal component used in many fields as communication, instrumentation, analog computing and control. It has one non-inverting input ($V+$), an inverting input ($V-$) and one output (V_{out}). There are also connections for a zero adjustment and the supply voltages $e-$ and $e+$. For this project we assumed a simple model for the OpAmp by presuming that the input currents $i+$ and $i-$ are zero and the output is given by the relation:

$$u_{out} = \text{sat}_{(u_{min}, u_{max})}(k(u_{+} - u_{-}))$$

and

$$\text{sat}_{(a,b)}(x) = \begin{cases} a, & \text{if } x < a \\ x, & \text{if } a \leq x \leq b \\ b, & \text{if } x > b \end{cases}$$

,while also assuming that the gain k is large and the next relation is satisfied:

$$e_{-} \leq u_{min} < u_{max} \leq e_{+}$$

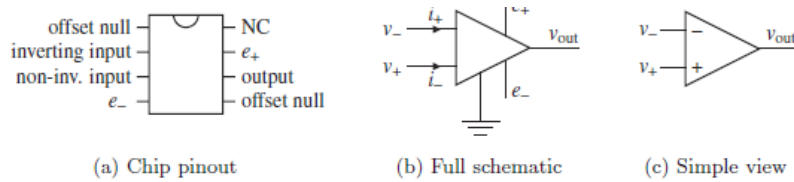
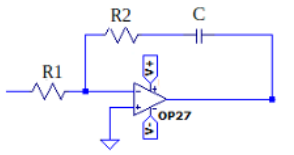


Figure 5.1: An operational amplifier and two schematic diagrams. (a) The amplifier pin connections on an integrated circuit chip. (b) A schematic with all connections. (c) Only the signal connections.

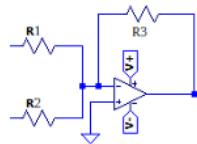
We can use that simple model of the OpAmp to sum and subtract signals but also implement the PI Controller. For the purpose of the thesis we use the OP27G model.

PI Controller



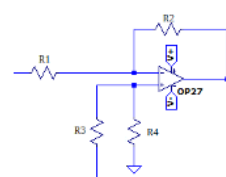
$$V_{out} = -\frac{R_2}{R_1} e(t) - \frac{1}{R_1 C} \int_0^t e(t) dt$$

Weighted Summer



$$V_{out} = -\left(\frac{R_3}{R_1} V_1 + \frac{R_3}{R_2} V_2\right)$$

Differential Amplifier



$$V_{out} = \frac{\left(\frac{R_2}{R_1} + 1\right)}{\left(\frac{R_3}{R_4} + 1\right)} V_3 - \frac{R_2}{R_1} V_1$$

(6) Voltage Control Oscillator

A voltage control oscillator is an electronic circuit which produces an oscillation with a frequency that depends on a control voltage. For the purpose of the thesis it is necessary to use an oscillator that generates a periodic signal with frequencies at the Radio Frequency (RF) spectrum (~MHz). We make use of the ZX95-100-S+ (Minicircuits) with linear tuning from 50 to 100MHz.

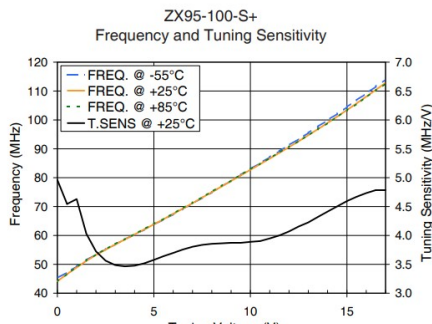


Figure 6.1

Outline Drawing

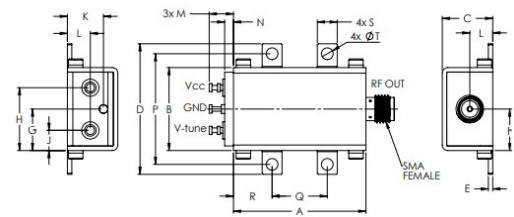


Figure 6.2

(7) Voltage Variable Attenuator

A voltage variable attenuator is an electronic circuit which attenuates an input signal based on a control voltage. For the purpose of the thesis we used the ZX73-2500+ (Minicircuits) capable of attenuating signal with frequencies between 10 and 2500Mhz.

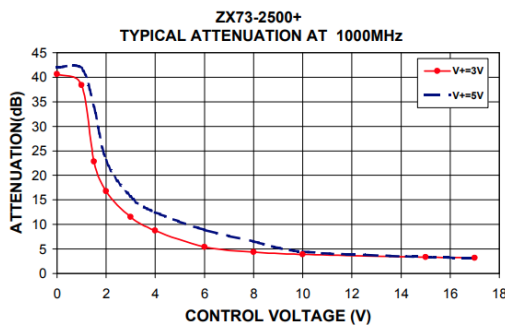


Figure 7.1

Outline Drawing (GD958)

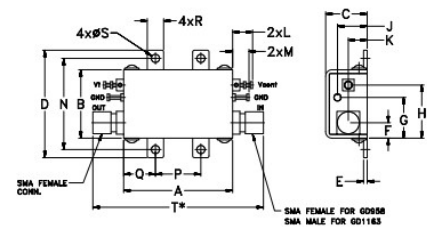


Figure 7.2

(8) Low Noise Amplifier

A low noise amplifier is an electronic amplifier which is capable of amplifying a very low-power signal without significantly degrading its signal to noise ratio. For the purpose of the thesis we use the ZX60-P103LN+ (Minicircuits).

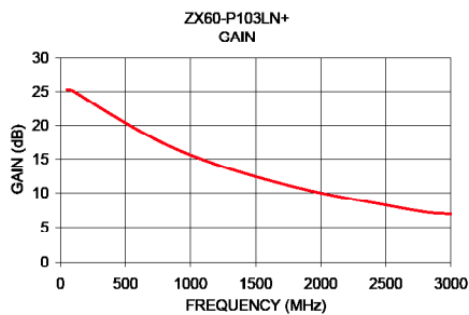


Figure 8.1

Outline Drawing

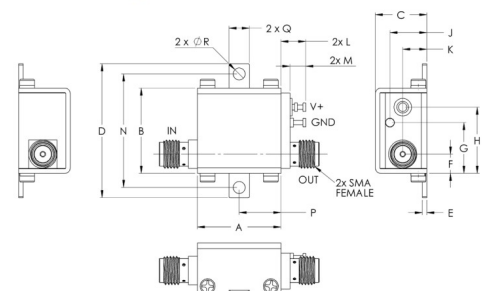


Figure 8.2

(9) Circuit design and symbolic circuit analysis

In this section we will make use of the principles of feedback and the Symbolic Circuit Analysis using the model of the ideal Operational Amplifier in order to design the control system and estimate its response, the Gain Margin and the Phase Margin. The output signal from the photodiode passes through a filter ($f_c \sim 10$ KHz) and reaches the differential amplifier. That signal is then subtracted from the Vset voltage (this is the reference voltage, the desired output from the

photodiode) and the result will be the error signal (the output of the differential amplifier). The error signal then passes through the PI controller and then a filter ($f_c \sim 10\text{kHz}$), which is one of the inputs of the weighted summer (U19). The necessity of the δV_{att} will be explained shortly, but first we will begin the symbolic circuit analysis analysis:

V_{pd} through -1 block:

$$V_{out_1} = -V_{pd} \quad (1)$$

V_{out_1} through F block:

$$\frac{V_{out_1} - 0}{R} = \frac{0 - V_{out_2}}{R} - C \frac{dV_{out_2}}{dt} \Rightarrow V_{out_1} = -V_{out_2} - R \cdot C \frac{dV_{out_2}}{dt}$$

from eq. (1):

$$V_{pd} = V_{out_2} + RC \frac{dV_{out_2}}{dt} \quad (2)$$

e through PI block:

$$\frac{e - 0}{R_1} = \frac{0 - V_c}{R_2} \Rightarrow \frac{e}{R_1} = -\frac{V_c}{R_2} \Rightarrow V_c = -\frac{R_2}{R_1} e \Rightarrow \frac{dV_c}{dt} = -\frac{R_2}{R_1} \frac{de}{dt}$$

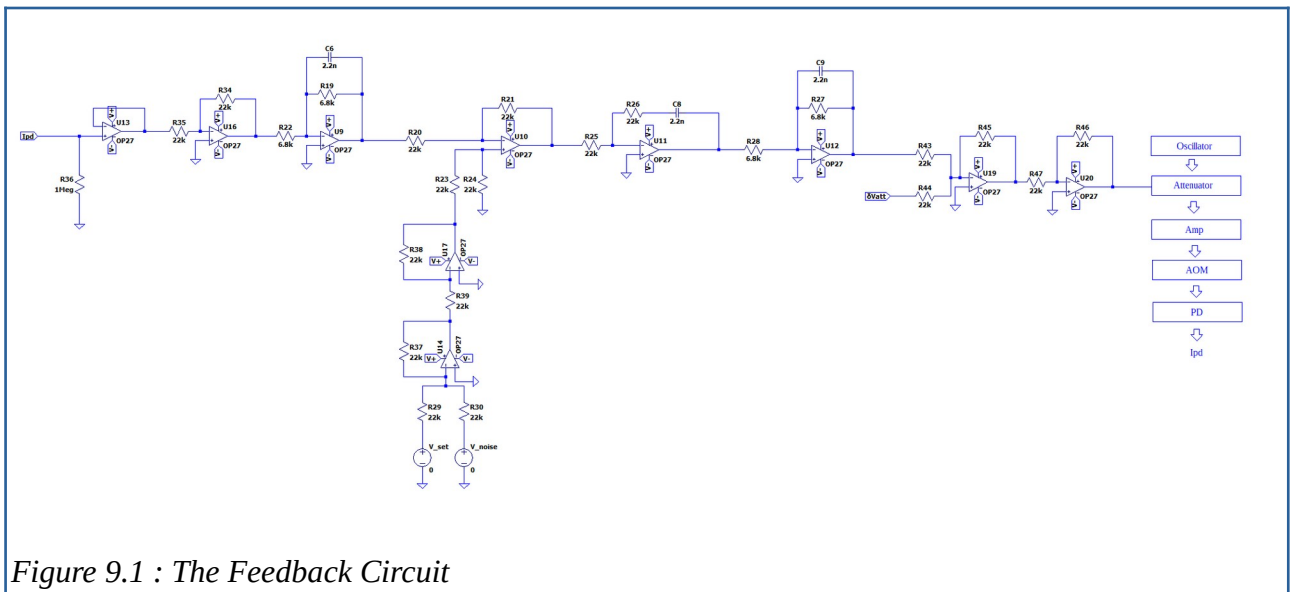


Figure 9.1 : The Feedback Circuit

$$\left. \begin{aligned} \frac{e-0}{R_1} &= C \frac{dV}{dt} \Rightarrow \frac{e}{R_1} = C \frac{dV}{dt} \\ V &= V_c - V_{out_3} \Rightarrow \frac{dV}{dt} = \frac{dV_c}{dt} - \frac{dV_{out_3}}{dt} \end{aligned} \right\} \Rightarrow \frac{e}{R_1} = C \left(-\frac{R_2}{R_1} \frac{de}{dt} - \frac{dV_{out_3}}{dt} \right) \Rightarrow$$

$$\Rightarrow e = -C R_2 \frac{de}{dt} - R_1 C \frac{dV_{out_3}}{dt} \Rightarrow \int_0^t e(t) dt = -C R_2 e(t) - R_1 C V_{out_3} \Rightarrow$$

$$V_{out_3} = -\frac{R_2}{R_1} e(t) - \frac{1}{R_1 C_i} \int_0^t e(t) dt \quad (3)$$

V_{out_3} through F block:

$$V_{out_3} = -V_{att} - RC \frac{dV_{att}}{dt} \quad (4)$$

Note: We studied the effect of the control voltage of the attenuator (V_{att}) independently by applying several values and measuring the V_{pd} . We have a feed-forward system that consists of the Oscillator, the Attenuator, the Amplifier, the AOM and the Photodiode (denoted by the blue block at Figure 9.1).

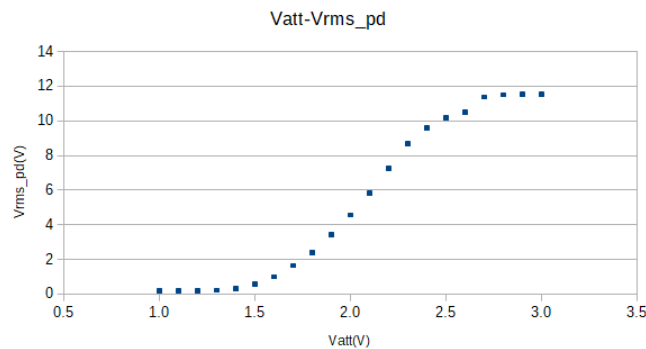


Figure 9.2: Voltage measurement as a function of the control voltage of the attenuator

When we attempt to lock the voltage of the photodiode at $V_{pd}=5V$, the control voltage of the attenuator is $V_{att}=2.316V$. We can perform a linear fit near that operating point (that way we may avoid the non-linear response that would make this analysis too complicated).

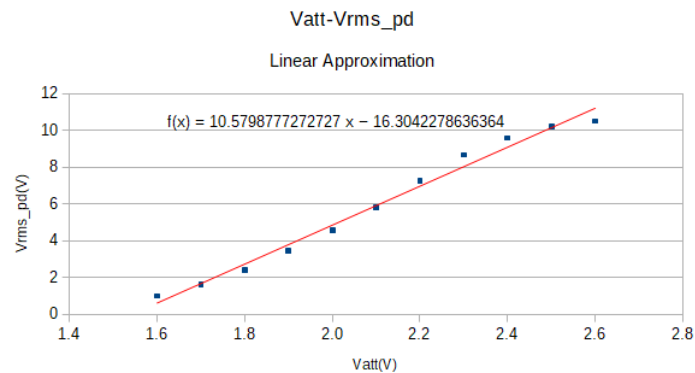


Figure 9.3: Linear Fit

We define the variables $A=10.58$ and $B=-16.30$ and as a result:

$$V_{pd} = A V_{att} + B \quad (5)$$

Even though we derived a linear equation for the variable V_{pd} and V_{att} , the system remains non-linear due to the constant B . We can define a new control voltage for the attenuator as:

$$V_{cnt} = V_{att} + \delta V_{att} \quad (6)$$

and by substituting (6) to (5):

$$V_{pd} = A(V_{att} + \delta V_{att}) + B \Rightarrow V_{pd} = A \cdot V_{att} + A \cdot \delta V_{att} + B$$

We can remove the term causes the non-linearity by assigning the voltage δV_{att} as :

$$\delta V_{att} = -B/A = 1.54 V$$

and a result we obtain:

$$\boxed{V_{pd} = A V_{att}} \quad (7)$$

$$\Rightarrow \frac{dV_{att}}{dt} = \frac{1}{A} \frac{dV_{pd}}{dt} \quad (8)$$

Substituting (8) to (4), (4) to (3), (3) to (2) and taking the time derivative and the Laplace transform we derive the Closed Loop Transfer Function:

$$\boxed{CLT = \frac{U_{out_2}}{U_s} = \frac{kp \cdot s + ki}{\frac{(RC^2)}{A} \cdot s^3 + \frac{2RC}{A} \cdot s^2 + (1/A + kp) \cdot s + ki}} \quad (9)$$

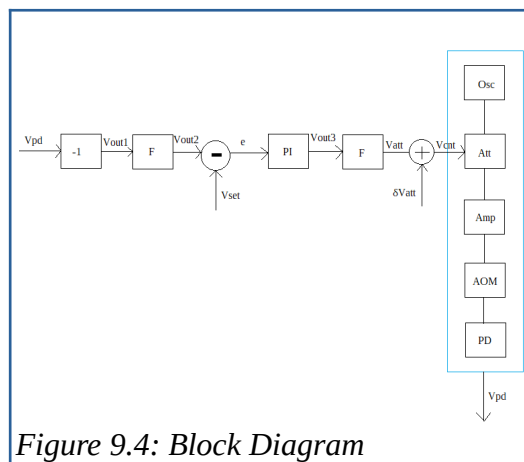


Figure 9.4: Block Diagram

We should also derive the Open Loop Transfer function as it is useful for determining the stability of the system:

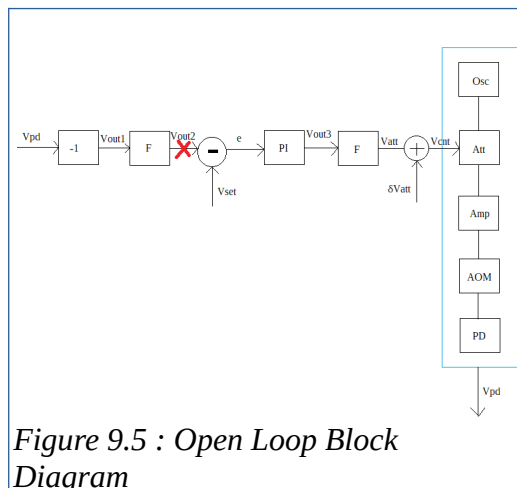


Figure 9.5 : Open Loop Block Diagram

By following the same steps we can derive the Open Loop Transfer Function as :

$$OLT = \frac{U_{out_2}}{U_s} = \frac{kp \cdot s + ki}{\frac{(RC^2)}{A} \cdot s^3 + \frac{2RC}{A} \cdot s^2 + \frac{1}{A} \cdot s} \quad (10)$$

and now we can easily observe that:

$$CLT = \frac{OLT}{1 + OLT} \quad (11)$$

Now we may use equation (11) to determine the Gain and Phase Margins via the Nyquist plot (using the python 3 library “Control”):

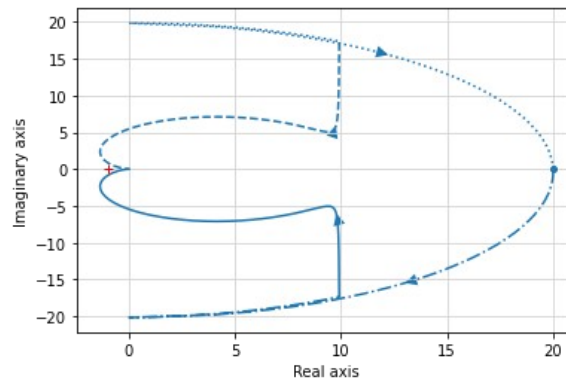


Figure 9.6: Nyquist Plot

$$GM = \text{infinite and } PM = 37.24^\circ$$

We managed to derive a transfer function for the system and create the Nyquist plot, but it is necessary to consider how accurate is that theoretical model. In order to derive the transfer function we assumed that the electrical components are ideal, which is not the case. We also assumed that we can break the feedback loop (to derive the OLT) by simply ‘cutting’ a wire, which is also an approximation since we are not taking into account the loading effect at the node. The previous statements combined with the large number of electrical components results in a model that approximates the behavior of the system and cannot accurately predict it. We may not expect the gain margin of the system to be infinite (as the Nyquist plot suggests) but we can expect it to be rather large. Thus the tuning will be performed experimentally and the stability of the system will be determined through measurement for different gains kp and ki .

(10) Measurements 1

A mechanical shutter is placed in front of the photodiode stays open (light reaches the photodiode) for 0.5s and is closed (no light reaches the photodiode) for 0.5s. The parameters of the PI controller: $R_1=R_2=22k\Omega$, $C=22nF$ and the reference voltage $V_s=5V$.

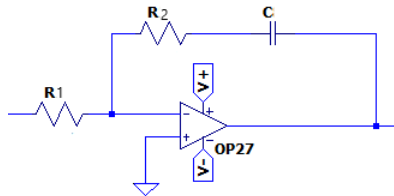


Figure 10.1: PI controller

As we can observe from the figure below there is a great overshoot 5V of short duration over the reference voltage and then the V_{pd} locks at 5V. This may be due to the large Loop-Gain, Proportional Gain or the Integral Gain and we have to investigate by changing each parameter individually.

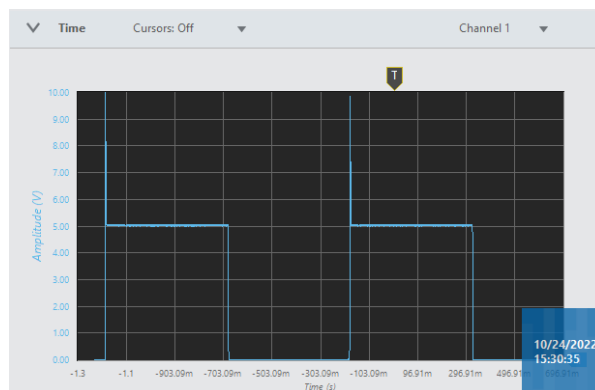


Figure 10.2: Tuning k_i

At first the proportional gain is reduced by a factor of 10 by replacing the $R_2=22k\Omega$ resistor with an $R_2=2.2k\Omega$. The resulting response is demonstrated in the graph below:

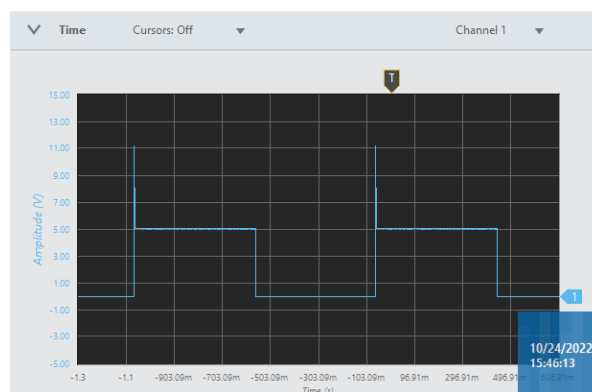


Figure 10.3

We observe that the reduction of the k_p gain had the opposite effect and increased the overshoot by $\sim 1V$. The resistor R_2 will be replaced with its initial value and the next step is to reduce the Loop-Gain.

Tuning Loop-Gain

We may reduce the Loop-Gain by increasing the value of the resistor R_1 . The resistance is increased from $22k\Omega$ to $220k\Omega$ and the response of the system is presented in the figure below:

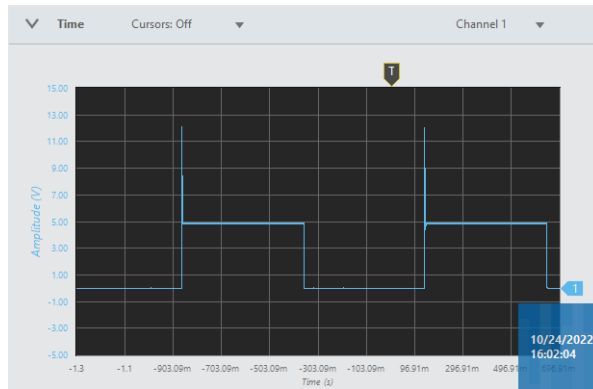
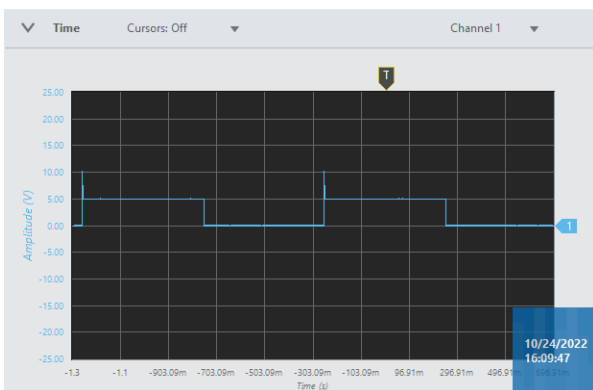


Figure 10.4

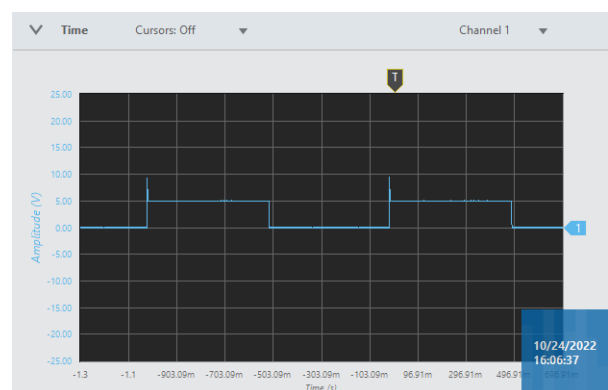
We observe that the reduction of the Loop-Gain had the opposite effect and increased the overshoot by $\sim 1.5V$. The resistor R1 will be replaced with its initial value and the next step is to reduce the k_i gain.

Tuning $k_i(2)$

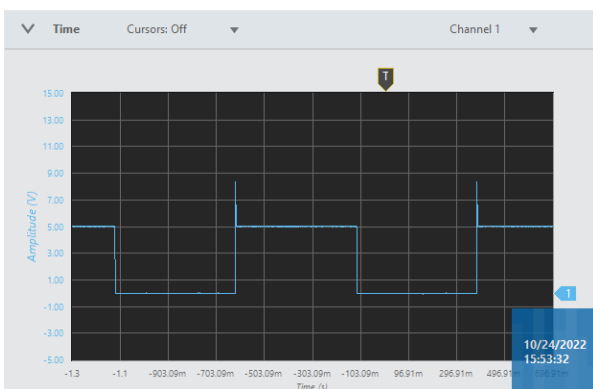
From the previous analysis we observe that the reduction of the Loop-Gain (lg), which reduces the k_p and k_i did not have desired effect on the response of the system. So instead of reducing the gain of the k_i controller we will reduce the time constant of the system by reducing the Capacitance. The response of the system for $C=10nF$, $C=5.6nF$, $C=2.2nF$ and $C=100pF$ is demonstrated:



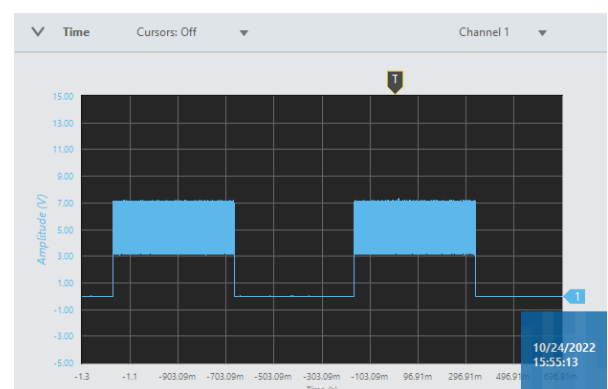
$C=10nF$



$C=5.6nF$



$C=2.2nF$



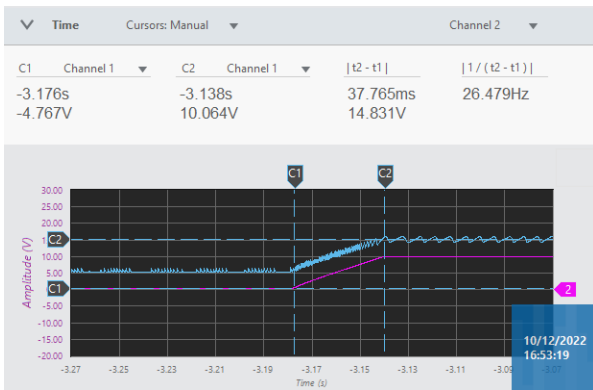
$C=0.1nF$

From the response of the system we determine that the problem that causes the overshoot are not the large gains k_i , k_p or lg , but the time response of the system. As the capacitance is reduced the k_i gain is increased but the overshoot is reduced. The cause of that problem is that the laser is open while the shutter is closed. As a result the feedback system has a constant error which tries to reduce. To do so the control voltage of the attenuator reaches its maximum value as an attempt to

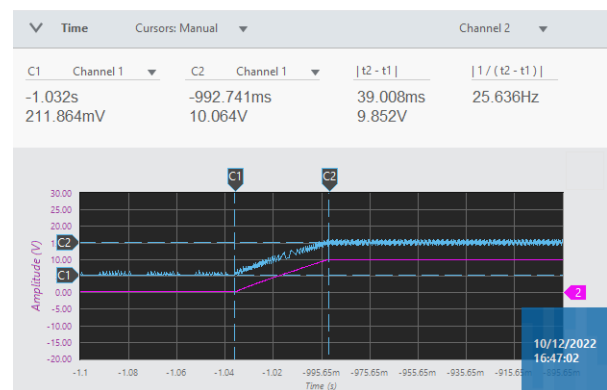
increase the light that reaches the photodiode(which is blocked by the shutter). The moment the shutter opens, for a brief time, the photodiode receives the maximum intensity that the system can provide, which is then reduced by the feedback system. Decreasing the time response of the system seems to reduce the overshoot but the system oscillates since the k_i gain is increasing(getting closer to instability). We can estimate that the overshoot is not a product of the poor tuning of the system. Another approach is to perform the experiment, and possibly confirm the previous statement for the tuning process, is to observe the response of the system the moment we set the reference voltage from 0 to 5V without the use of a shutter.

(11) Measurements 2

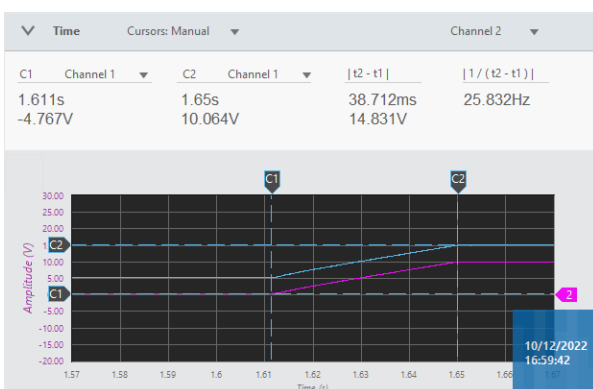
This time we will perform the same experiment but without the use of a shutter and the response of the system will be observed by changing the reference voltage from 0 to 10V. Since laser remains open(even if the reference voltage is zero) some light will reach the photodiode ($\sim 150\text{mV}$) but we do not expect that will effect the response. The resistors of the controller have the same value of $22\text{k}\Omega$ and the capacitance is varying, with the results presented bellow: (the blue line is the photodiode voltage and the purple line is the reference voltage)



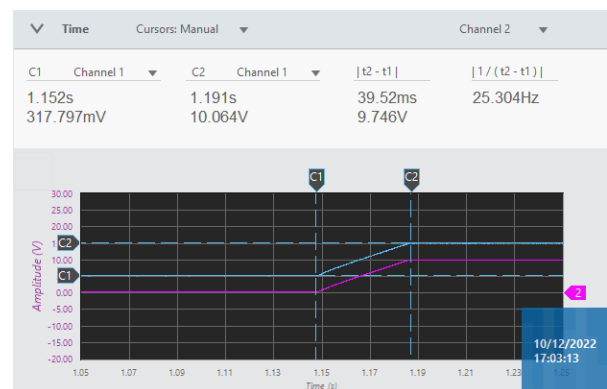
2.2nF



5.6nF



22nF

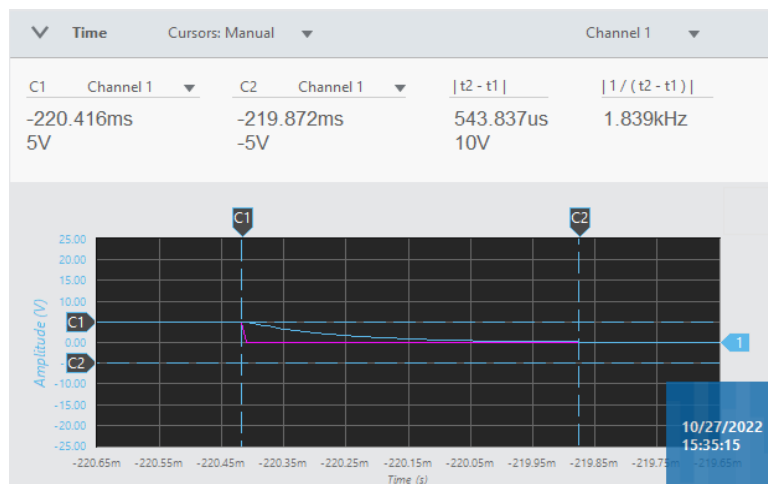
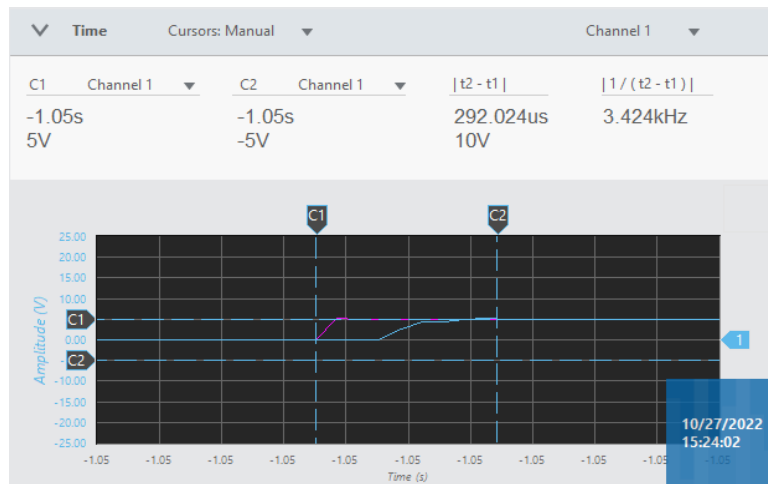
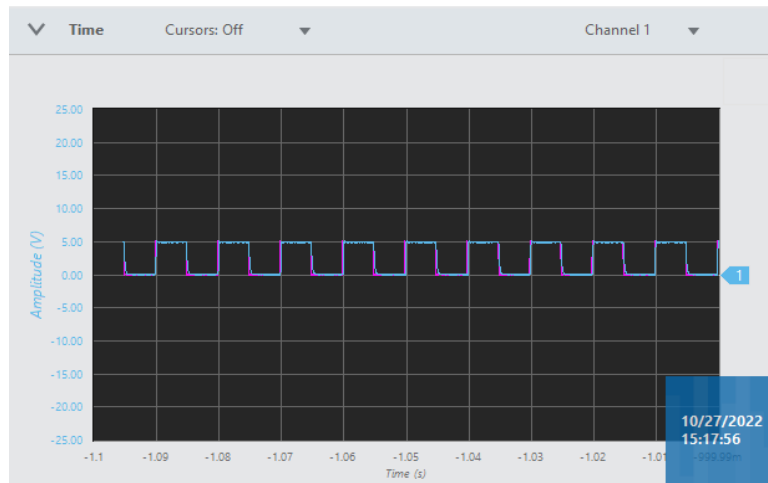


44nF

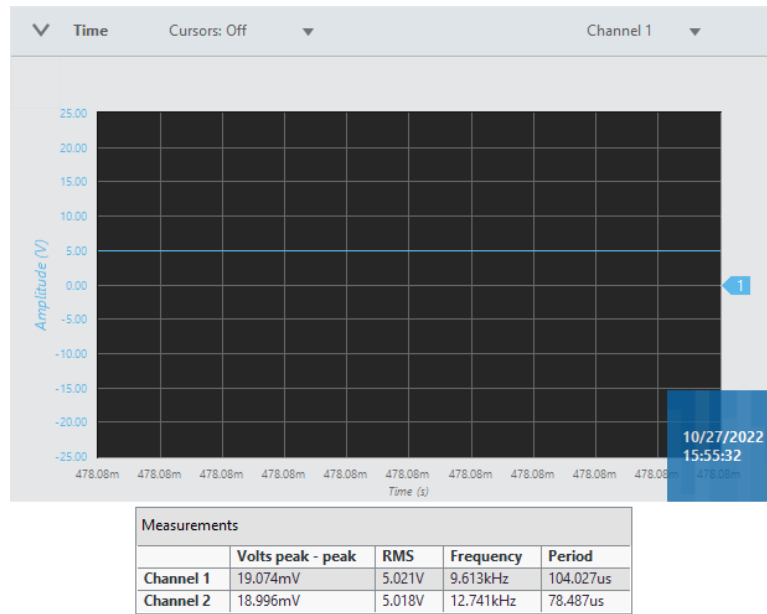
As we can observe we eliminated the overshoot and we can also observe that with increasing capacitance we also eliminate unwanted oscillations. We may solved the previous problem but another arise, the voltage source is not really a pulse, but a ramp signal which means that it has a large rise time. The desired response of the system must be in the range of 1ms. We can replace the analog voltage source with a function generator that provides square pulse and repeat the same

process, the results are presented below for V_s a square pulse signal $V_{pp}=5V$, $D_{offset} = 2.5V$ and frequency of 100Hz.

Note: The blue line represents the voltage of the photodiode and the purple line the V_s (reference voltage).



We are able to lock the pulse at the desired reference voltage with a rise time of $t=292.024\mu s$ and when to V_s drops to zero volts the photodiode voltage falls with $t=543.837\mu s$. The PI parameters are: $R1=10.84k\Omega$, $R2=13.88k\Omega$ and $C= 5.6nF$. Now we will set the voltage to 5V DC and observe what happens at the steady state:



Channel 1: Photodiode
Channel 2: Vs

(12) Experimental set-up of the optical components 1

A laser diode (ThorLabs LDC205C) 532nm is placed in-front of an acousto-optic modulator(AOM ISOMET 1205c-1). The AOM uses the acousto-optic effect to diffract the incident light and also shift its frequency. The light that passes through the AOM is diffracted and the diffraction pattern is described by the formula bellow:

$$2 \Lambda \sin \theta = m \frac{\lambda}{n} ,$$

,where λ is the wavelength of light in vacuum, $m=...,-1,0,+1,...$ is the order of the diffraction, Λ is the wavelength of the sound and n is the refractive index of the crystal. The intensity of the sound modulates the intensity of the diffracted beam. The formula for the efficiency for $m=+1$ is presented bellow:

$$\eta = \frac{I_1}{I} = \sin^2 \left(\frac{\Delta \phi}{2} \right)$$

where the external phase excursion: $\Delta \phi = \frac{\pi}{\lambda} \sqrt{2 \left(\frac{L}{H} \right) M_2 P}$.

A lens is placed in after the AOM to focus the diffracted light. We use the first order of diffraction to modulate the intensity of the beam by placing an iris to block the rest orders of diffraction. Light then reflects on tow mirrors(the plane of its mirror is at 45 degrees to the incident light so the experimental set-up creates a 'π' like shape), passes through a second lens and finally reaches the photodiode(ThorLabs DET36A2). The out output of the photodiode is a current so by placing a resistor that is connected to the ground(and the buffer of the control circuit) we invert current to voltage. A 1MΩ resistor is placed so the output frequency bandwidth is ~4kHz derived from the formula that is given from the manufacturer:

$$f_{BW} = \frac{1}{(2\pi R_{LOAD} \times C_j)}$$

(13) Pulse repeatability

We set a function generator to generate a square pulse at 1Hz with amplitude of 5V(for 100ms V=5V and for 900ms V=0V ,dt=1ms per measurement) and collect data to observe if the number of photon per pulse is the same or deviates with time.

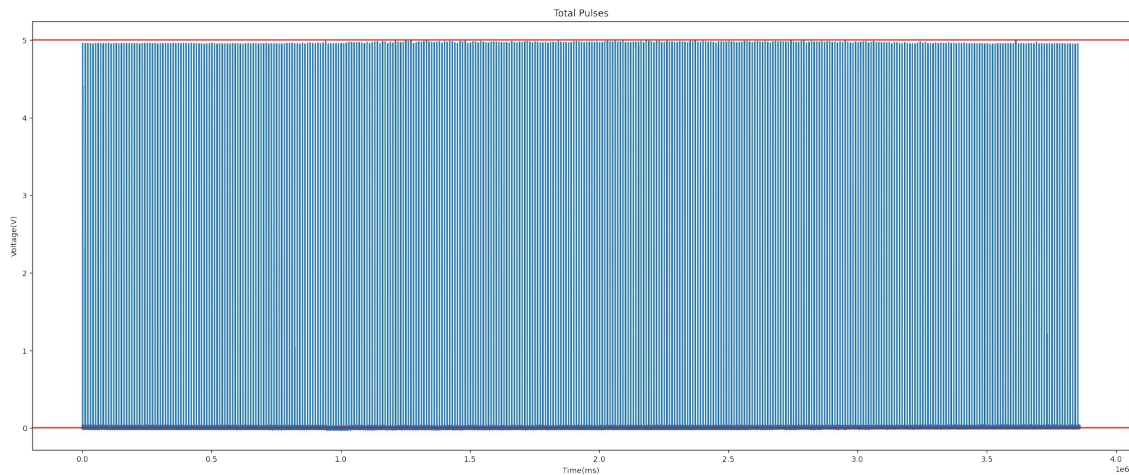


Figure 13.1: Generated pulses over time

We can attempt to reduce the time step of the measurement from 1ms to 100μs so that way we may increase the precision of our measurements. We collect data for 24 pulses (we perform 5 different measurements, four for five continuous pulses and one for four continuous pulses and each measurement is performed at random time). Then we merge the data to perform the integration:

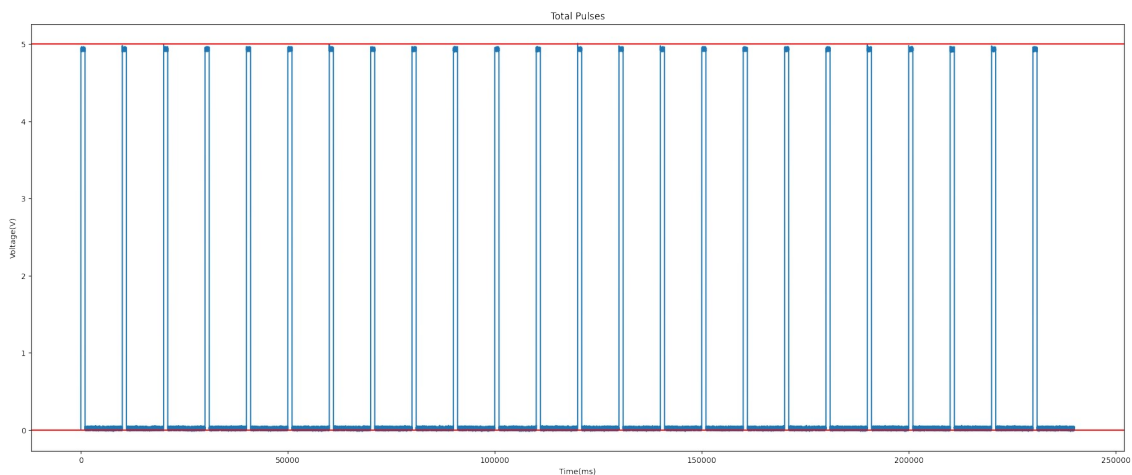


Figure 13.2 : Generated pulses with reduced time step

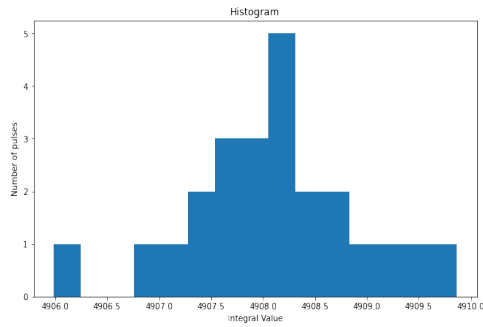


Figure 13.3 : Histogram

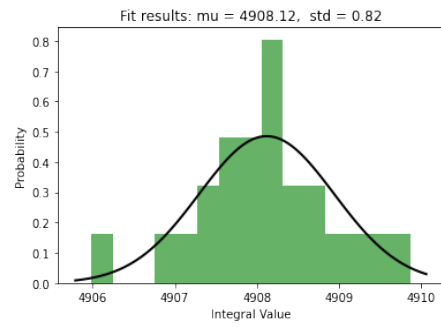


Figure 13.4: Mean Value and Standard Deviation

It is not hard to prove that the total number of photons per pulse is proportional to the time integral of the Voltage we measure. We can begin with the formula for the number of incident photons per second for a free space photodiode:

$$N_p = \frac{P_\lambda}{hc/\lambda}$$

, P_λ is the power of the incident beam that interacts with the photodiode and λ_0 is the wavelength of the monochromatic beam. The responsivity of the photodiode is given by the following formula:

$$R(\lambda) = \frac{I_{PD}}{P_\lambda}$$

, I_{PD} is the generated photocurrent.

We can solve the second equation for P_λ and replace that term on the first formula, resulting to:

$$N_p = \frac{I_{PD}}{R(\lambda)} \left(\frac{\lambda_0}{hc} \right)$$

In the Figure 1.5 it is shown that the output of the photodiode is connected to a resistor, which is connected to the ground, and the non inverting input of an OpAmp(the buffer). By measuring the voltage we can determine the generated photocurrent I_{PD} as:

$$I_{PD} = \frac{V_{PD}}{r}$$

and as a result we conclude that the number of incident photons per second is given by:

$$N_p = \frac{V_{PD}}{r \cdot R(\lambda)} \left(\frac{\lambda_0}{hc} \right)$$

Now we can integrate:

$$\tilde{N}_p = \frac{1}{r \cdot R(\lambda)} \left(\frac{\lambda_0}{hc} \right) \int_{t_0}^{t_1} V_{PD} dt$$

With a standard deviation of $std = 0.82$ we expect 99.7% of the pulses to lie within 3 standard deviations of the mean (or 0.05% percentage deviation from the mean value).

The feedback system that makes use of the AOM provides an easily tuned and repeatable pulse over time. Now we can continue to the second part of the thesis and use the control system to shine light on the pupil and observe the pupillary reflex.

(14) Basic anatomy and function of the eye

Pupils react to three different kinds of stimulation: pupil light response(they constrict in response to increased brightness and dilate due to decreased brightness), pupil near response(or “adjustment to close-range vision” that results to constriction due to near fixation), and the response to increased mental effort and arousal(results to dilation of the pupil). We are interested in the first kind also known as PLR since we intent to shine light on the pupil and measure its response.

Anatomy

The pupil is located at the center of the eye and is a transparent opening. The pupil exposes the lens and light passes through its surface which is then focused at the back of the eye, onto the area called the retina. Since the inside of the eye is dark, the pupil appears black(that means that it is not an opaque black surface).The pupil can effect the quantity of light that enters the eye by a factor of 16 since its diameter varies in the range 2-8mm.

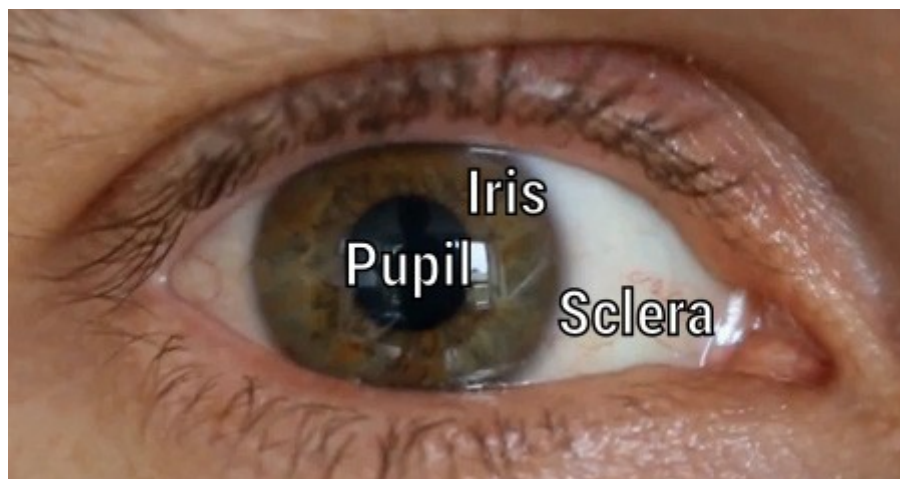


Figure 15.1 : The human eye

The iris contains the muscles that change the pupil diameter, and is the distinctive colored area around the pupil. On top of the iris and pupil, the cornea is located, which is a transparent tissue that refracts light and allows it to enter the eye. Lastly the white area around the iris is the sclera and covers most of the outside of the eyeball.

Neural pathways

Tow neural pathways control the pupil size, the parasympathetic constriction pathway and the sympathetic dilation pathway. The constriction and dilation pathways are interconnected but are often considered distinct.

The constriction pathway

The iris sphincter muscle is the one responsible for the pupil constriction. It encircles the pupil and reduces its size(of the pupil) when it contracts. The parasympathetic nervous system is a part of the autonomic nervous system and innervates the iris sphincter. The constriction pathway is the link

between the iris sphincter muscle and the retina, and belongs to the category of the sub-cortical pathways.

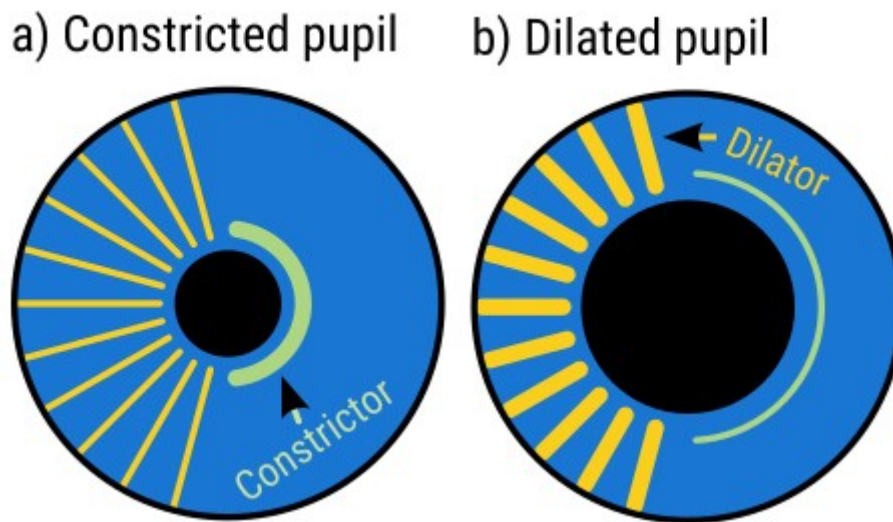


Figure 15.2: The constricted and dilated pupil

When light falls onto the retina, nerve impulses travel along the optic nerve to the optic chiasma (which is the part of the brain where the optic nerves cross). Then the optic chiasma combines the information from the retina of both eyes, re-organizes it based on the visual field, and sends it to the pretectal nucleus (PN). Information from the right eye travels to the PN of the left hemisphere and information from the left eye travels to the PN of the right hemisphere. The information then is sent to the Edinger-Westphal nucleus (EWN) which contains a group of parasympathetic cells that supply with nerves the ciliary (responsible for the eye movement) and sphincter muscles. From the EWN, information travels to the ciliary ganglion (CG) via the Oculomotor Nerve and then to the iris sphincter muscle.

The dilation pathway

The iris dilator muscle controls the pupil dilation. The dilator muscle is composed of fibers, radially oriented, that connect the interior with the exterior of the iris. When the muscle contracts the interior of the iris is pulled outwards, and that results to the increase of the pupil area. The sympathetic nervous system, which is a part of the autonomic nervous system that is involved in the fight-or-flight response and wakefulness, controls the iris dilator muscle. That link between the sympathetic nervous system and the pupil explains why the pupil dilates when someone is stressed. The dilation pathway is a subcortical pathway that begins at the locus coeruleus (LC) and the hypothalamus (which is a complicated structure with many connections) and connects to the iris dilator muscle. LC reflects arousal since it is particularly active when an organism is alert, aroused or awake and the hypothalamus reflects arousal and wakefulness. Both the hypothalamus and LC project to the intermediolateral column (IML) of the spinal cord and the IML itself projects to the superior cervical ganglion (SCG) outside of the spinal cord. The SCG then projects via number of nerves to the iris dilator muscle.

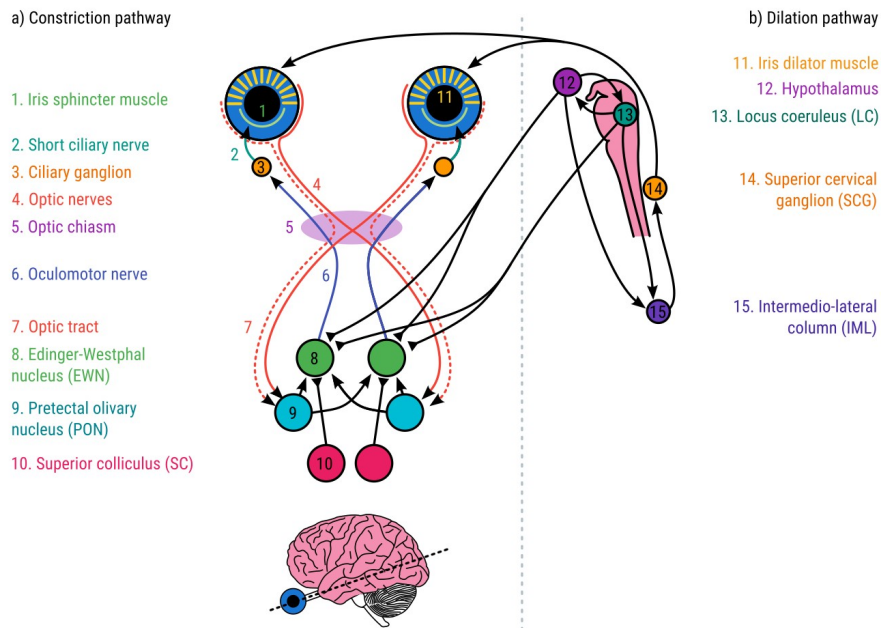


Figure 15.3: The Constriction and Dilation pathways

The pupil light response

The pupil light response (PLR) is the dilation of the pupil due to darkness and the constriction of the pupil in response to brightness. A common PLR is presented at Figure 15.4, resulting from 10s of red or blue light followed by 20s of a dark screen.

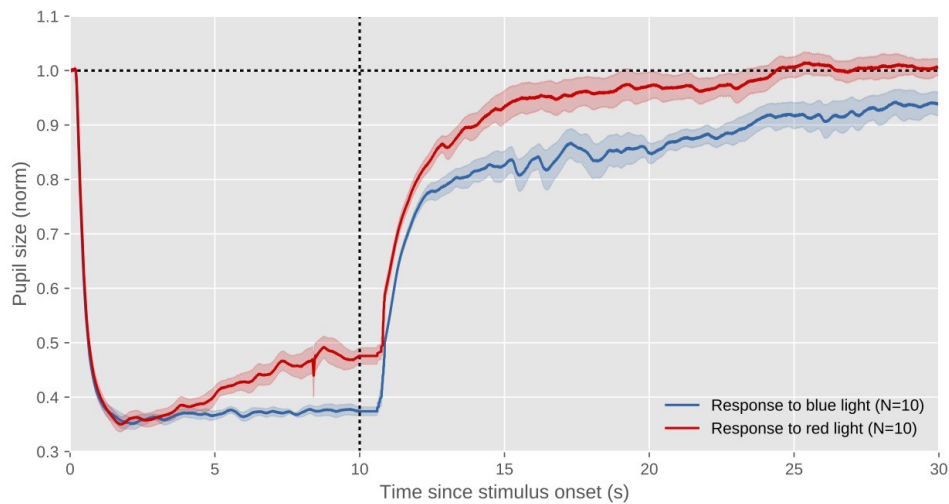


Figure 15.4: Profile of typical PLR response

Typical PLR response over time:

- Light on/0.0 – 0.2s: The pupil does not respond yet and the latency depends on several factors such as the intensity of the light and the age of the test subject.
- Light on/0.2 – 1.5s: The pupil constricts rapidly until it reaches its minimum size.
- Light on/1.5 – 10s: The pupil either dilates slightly or remains constricted while light continues to shine on the eye. This dilation of the pupil is often called pupil escape and depends on the color of the light (this is a result of different photoreceptors for the blue and red light).

-Light off/10s – 30s: The pupil returns over time to its original size. The dilation process occurs much more slowly and it can take several minutes for the pupil to return to each original size. This process is slower for the blue light(in comparison to the red light). It is worth noting that after high – intensity blue light the pupil remain constricted for several minutes and this phenomena is called post – illumination pupil response(PIPR).

Pupil reflex as a control system

Since the pupil constricts and dilates depending on the light flux that interacts with the retina, we can approach the system of the pupil reflex as a simple feedback control system described by the block diagram bellow:

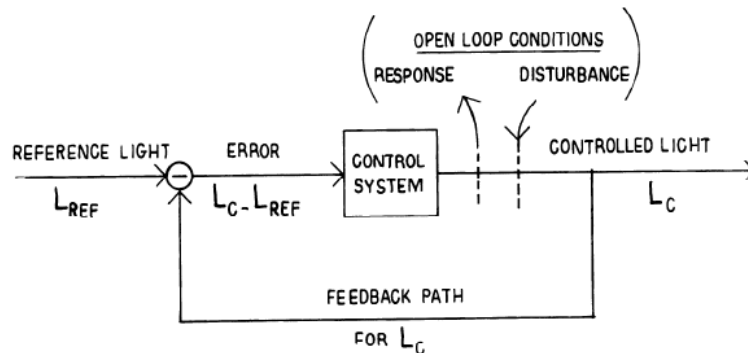


Figure 15.4: Simple control system

We can assume a reference flux (L_{ref}) that it is always compared with the actual flux (L_c) interacting with the retina. The L_c is the controlled variable since by constriction or dilation of the pupil, the amount of light passing though the pupil decreases or increases. Naturally the error signal of the control system is $L_c - L_{ref}$. The controller changes the pupil size so error is minimized.

(15) Experimental set-up and measurements

In the previous sections we designed and implemented a feedback circuit with a PI controller for the intensity and the pulse shape of a laser using an AOM, and later introduced the basic anatomy of the eye and how it functions as a feedback control system. In this section we will present how the PI controller can be combined with a set of optical components so we can perform measurements for the pupillary reflex. The first component of the set-up is a 532nm laser (green) which provides the stimulus. The laser beam goes through the AOM which modulates the intensity for every order of diffraction, but for the measurements we only make use of the first which goes through the first fiber coupler. Besides the 532nm laser, an 850nm laser is implemented in the set-up. The human eye is not sensitive to infra-red(IR) light and as a result it does not stimulate it, so we can use reflected IR from the eye to capture images. Therefor the 850nm beam goes through the second fiber coupler and the tow beams are fiber coupled into the fiber combiner, resulting to superimposed colors on common spatial mode. After the fiber collimator, a thin microscopy glass is placed to reflect a small amount of the beam to the photodiode. Since we need to modulate only the stimulus light after the fiber output, the light that interacts with the photodiode of the feedback system must be comprised only of the 532nm light(and that because the photodiode is also sensitive to IR light which fluctuates due to the fiber). To do so a dichroic lens is placed before the photodiode to reflect the 850nm and transmit only the 532nm light. In the section (10) of the thesis it is stated that timing of the V_{ref} and the triggering of the shutter is important since it effects the response of the system, and the problem being the time delay for the shutter to fully open. To counter that effect we can set a pulse to activate the shutter 15ms before the pulse of the stimulus light. That way shutter does not

effect the stimulus light but also make sure that no light interacts with the eye when the V_{ref} is zero volts (the AOM can not completely eliminate the intensity of the light and as a result when we set V_{ref} to zero a small amount of the 532nm passes through the fiber). The light then passes through a beam expander, and expands to a diameter about 3cm, and an LCD that provides the pattern controlled via the computer. Eventually the light goes through a beam splitter so half of the beam goes through a lens and stimulates the eye and the IR is reflected back to the beam splitter and reaches the camera.

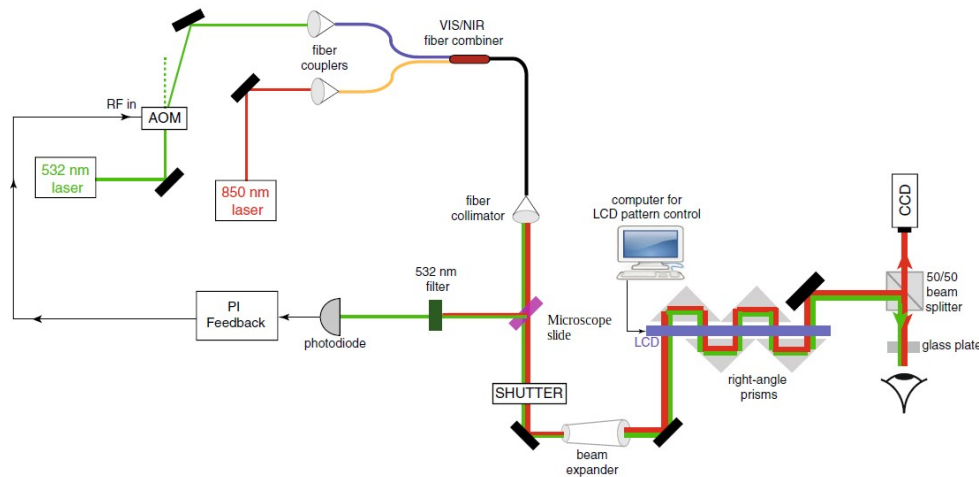


Figure 15.1: Experimental apparatus

The LCD can provide several patterns, but for this measurement only one central pixel is active. We are interested in the indirect pupil reflex, which means that only one eye is illuminated (right eye) and the response (if any) of the other will be observed. After dark adaptation for ten minutes, the right eye is illuminated for 100ms the responses of both eye are recorded by the cameras (117fps). The following figures depict the pupil before the stimulus, during the stimulus and after the constriction of the pupil (for the measurements the IR beam was not in use). We also make use an infrared lamp (the eye is not sensitive to that wavelength as stated before) above the eyes so that way we may have a clear image for extract information.



Figure 15.2: Pupil before stimulus (Right eye)



Figure 15.3: Pupil during stimulus(Right eye)



Figure 15.4: Constricted pupil(Right eye)

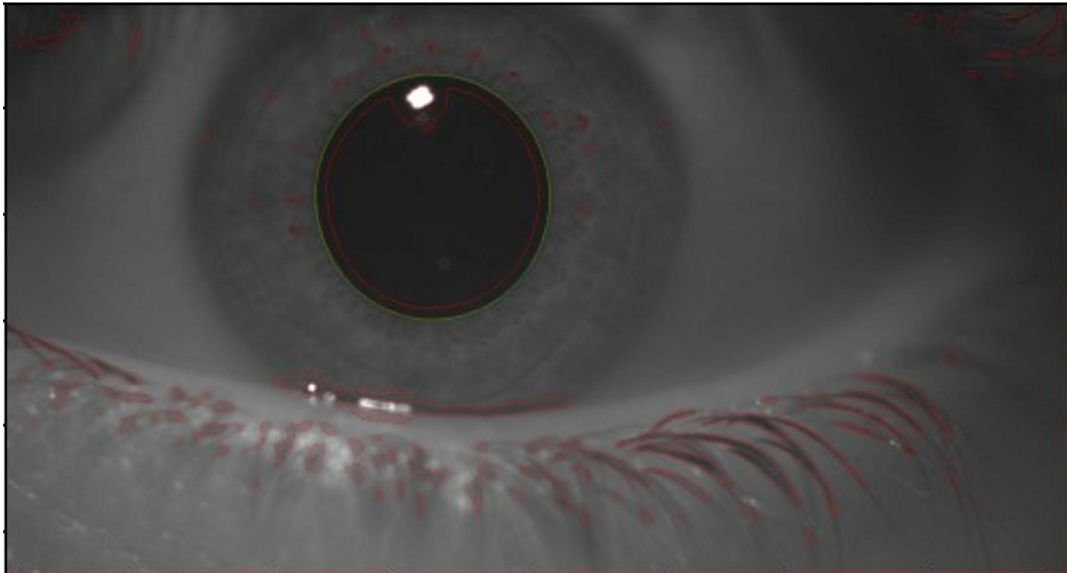


Figure 15.5: Contour of the pupil

The images that were captured are processed by an edge detection algorithm (provided by my colleague Chrysafi Emmanouela) that is capable of determining the area of the pupil based on the sudden change in pixel intensity at the boundaries of the iris and the pupil (the iris is significantly brighter than the pupil). The algorithm then fits an ellipse around the pupil and calculates its area. The base arbitrary unit for all the measurements is pixel number, and that is an important detail that will be discussed later. The graphs of the pupillary reflex for both eyes are demonstrated below:

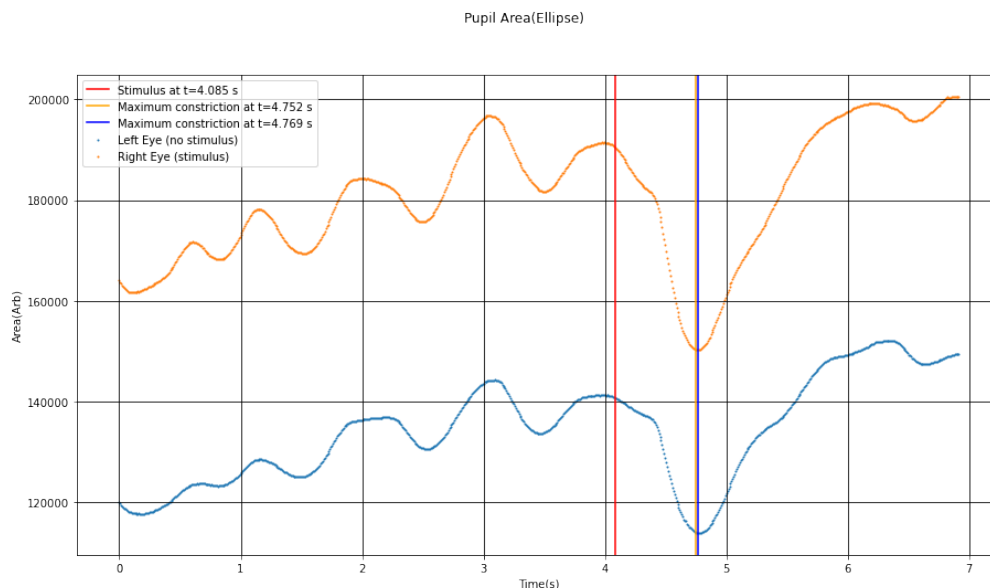


Figure 16.5: Pupillary reflex

As we can observe from the data, the pupil of the left eye (no stimulus) responds to the stimulus of the right eye. The reason we observe the indirect pupillary reflex may be the optic chiasma of the constriction pathway which combines information from both eyes as explained in the previous section. The camera captures 2048x1088 pixel image and the algorithm measures distances in pixel

number so the current method of calculating the pupil area and the values that the algorithm returns depend on the camera focus which differs for every eye and as a result we can not compare the sizes of the pupil. Since the system is not calibrated we can instead normalize each data sets(for the left and right eye) by dividing the data with the first area(first frame) that the algorithm returns. That way we can determine how the pupil area changes relatively to the initial area at the start of the measurement:

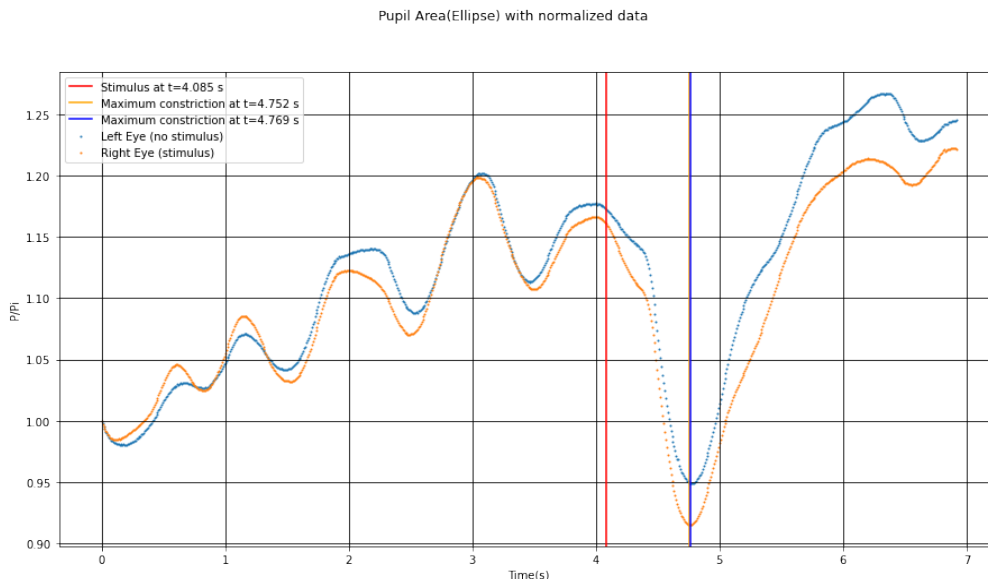


Figure 16.6: Pupillary reflex with normalized data

Lastly we can also determine the percentage of the change for the pupil area relatively to the area at the time of the stimulus:

Percentile Divination	
Right Eye	21.16%
Left Eye	19.07%

It has to be noted that the cameras record at 117fps which means that a measurement occurs every ~ 0.0085 ms. The recording begins before the eyes are open while the infra-red lamp is turned off. As soon as the eyes are open, the infra-red lamp is turned on so we can record the pupil response. As a result of that process, we define the beginning of the measurement for its data-set(individual data-set for each eye) the first frame that is not dark(the frames are dark due to the lack of reflected IR light from the eye). That process, combined with the fact that the recording for each camera does not begin at the same time, results to an uncertainty of ~ 0.00425 ms for time difference between the first data point between the two data-sets. In other words the absolute time of capture of first image of one data-set may differ from the absolute time of capture of the second image a time from 0s-0.00425s. That is important because we can not accurately make a statement for the phase difference between the graphs.

(16)Pupillometry- Application in medicine and Challenges

Pupillometry has become a subject of great interest, especially in the field of medicine, since several studies attempt to correlate the PLR to diseases relevant directly to the eye or the parasympathetic and sympathetic nervous system. For example glaucoma is a usual eye condition which is caused by elevated intraocular pressure(IOP) and result to optic nerve damage. If this condition is left unchecked it can lead to partial loss of sight and even blindness. Glaucoma patients often suffer from cardiac autonomic dysfunction(CAN) which is related to the parasympathetic and sympathetic nervous system. Thus the diagnosis of autonomic dysfunction may be the means for the prognosis and treatment for glaucoma. Another example is the Parkinson's diseases that effects the sympathetic and parasympathetic nervous system. Although the study of PLR seems promising(especially with modern experimental equipment to perform the measurements and machine learning to analyze the data) there are also great challenges ahead. Since the PLR is a poly-parametric phenomena (it is related to eye diseases, diseases of the parasympathetic and sympathetic nervous system and even the psychological state of the subject) it is a challenge to find a large group of patients that mach the criteria necessary to perform measurements in a large scale but it is also a challenge to accurately correlate the PLR response directly to a disease.

Bibliography

- [1]: Karl Johan Astrom, Richard M. Murray (2019-08-18). Feedback Systems An introduction for Scientist and Engineers
- [2]: Park, H.Y.L., Jung, S.H., Park, S.H. and Park, C.K., 2019. Detecting autonomic dysfunction in patients with glaucoma using dynamic pupillometry. *Medicine*,98(11).
- [3]: Margaritakis, A., Anyfantaki, G., Mouloudakis, K.*et al.* Spatially selective and quantum-statistics-limited light stimulus for retina biometrics and pupillometry. *Appl. Phys. B* 126, 99 (2020). <https://doi.org/10.1007/s00340-020-07438-z>
- [4]: Lawrence Stark and Philip M. Sherman. A SERVOANALYTIC STUDY OF CONSENSUAL PUPIL REFLEX TO LIGHT. *Journal of Neurophysiology* 1957 20:1, 17-26
- [5]: Wilson John, Hawkes John (2014). Optoelectronics: An Introduction (3rd Edition) University Press N.T.U
- [6]: Evangelia Giza, Dimitrios Fotiou, Sevasti Bostantjopoulou, Zoe Katsarou & Anna Karlovasitou (2011) Pupil Light Reflex in Parkinson's Disease: Evaluation With Pupillometry, *International Journal of Neuroscience*, 121:1, 37-43, DOI: 10.3109/00207454.2010.526730
- [7]: Adel S. Sedra, Kenneth C. Smith. Μικροηλεκτρονικά Κυκλώματα, Τόμος Α (7η έκδοση)(2017)
- [8]: Mathôt, S., 2018. Pupillometry: Psychology, physiology, and function. *Journal of Cognition*, 1(1).